International Journal of Research in Engineering and Science (IJRES)
ISSN (Online): 2320-9364, ISSN (Print): 2320-9356
www.ijres.org Volume 7 Issue 8 ǁ 2019 ǁ PP.13-24

Osseointegrative, Angiogenic and Antiinfective Properties of Magnesium-Modified Acrylic Bone Cement

Mangalashrita Parida, Soumya Ranjan Rath, Jyotirmayee Panda,Bipas Mohanty
Department of Civil Engineering, NM Institute of Engineering and Technology,Bhubaneswar , Odisha
Department of Civil Engineering, Raajdhani Engineering College,Bhubaneswar,Odisha
Department of Civil Engineering,Aryan Institute of Engineering and Technology Bhubnaeswar , Odisha
Department of Civil Engineering,Capital Engineering College,Bhubaneswar,Odisha

Abstract
This work centers around handling the insufficient bone/embed interface strength of acrylic bone concretes, which is an impressive issue reducing their clinical per-formance, particularly in percutaneous kyphoplasty medical procedure.
Methods*: A new strategy of incorporating magnesium particles into clinically used poly(-methylmethacrylate) (PMMA) bone cement to prepare a surface-degradable bone cement (SdBC) is proposed and validated both in vitro and in vivo.*
Results: This surface degradation characteristic enables osseointegrative, angiogenic and anti- infective properties. SdBC showed fast surface degradation and formed porous surfaces as de- signed, while the desirable high compressive strengths (≤70 MPa) of the cement were preserved. Besides, the SdBC with proper Mg content promoted osteoblast adhesion, spreading, proliferation and endothelial cell angiogenesis capacity compared with PMMA. Also,SdBC demonstrated clear inhibitory effect on Staphylococcus aureus and Escherichia coli. In vivo evaluation on SdBC by the rat femur defect model showed that the bone/implant inter-face strength was significantly enhanced in SdBC (push-out force of 11.8 T 1.5 N for SdBC vs suggesting significantly improved osseointegration and bone growth induced by the surface degradation of the cement. The injectability, setting times and compressive strengths of SdBC with proper content of Mg particles (2.8 wt% and 5.4 wt%) were comparable with those of the clinical acrylic bone cement, while the heat release during poly-merization was reduced (maximum temperature 78 T 1 °C for PMMA vs 73.3 T 1.5 °C for SdBC).
Conclusions: This work validates a new concept of designing bioactive bone/implant interface in PMMA bone cement. And this surface-degradable bone cement possesses great potential for minimally invasive orthopaedic surgeries such as percutaneous kyphoplasty.
The translational potential of this article: This work reports PMMA/Mg surface-degradable acrylic bone cements that possess enhanced osseointegrative, angiogenic and antiinfective properties that are lacking in the clinically used acrylic bone cements. This new kind of bone cements could improve the treatment outcome of many orthopaedic surgeries such as percu- taneous kyphoplasty and arthroplasty.
KEYWORD: *Antiinfection;Bone cement;Kyphoplasty;Magnesium;Osseointegration:*

I. INTRODUCTION

Poly(methylmethacrylate) (PMMA)-based bone cements have been widely used in the current orthopaedic surgeries, including arthroplasty, treatments of femoral head osteonec- rosis and spinal degenerative diseases. The fast polymeriza- tion and injectable capability of PMMA gives bone cement numerous advantages over preshaped implants, especially for the applications in the minimally invasive orthopaedic surgery (MIOS) such as percutaneous kyphoplasty (PKP) and verte- broplasty (PVP) [1,2]. Nevertheless, the need for improving PMMA rises because a large number of clinical cases indicate the risks of excessive heat released from acrylic monomer polymerization [3] and inadequate strength at the bone/

cement interface, causing the instability of the interface or failure of the bone bonding to cement clump [4e7]. The inadequate interface strength was attributed to the lacks of osseointegrative and biodegrading ability of PMMA [8e10]. Modification of PMMA by incorporating bioactive or biode- gradable additives has shown great potential to tackle these two problems simultaneously [9e13].

In addition, on the one hand, angiogenic capabilities become highly desirable for next-generation bone cement. Angiogenesis is critical for bone growth and regeneration, especially for diseases such as osteonecrosis. It is important for bone regeneration to build up a functional vascular network within the defect site, which can provide sufficient oxygen and nutrients to facilitate growth, differentiation and tissue functionality [14]. Also, the vascular invasion could reduce the risk of osteonecrosis around the bone substitutes. Angiogenic induction by bone cements itself is therefore a simple and efficacious strategy for bone regeneration and osteonecrosis prevention, which are important for enhancing strength at the bone/PMMA interface. On the other

hand, bone cementerelated infection has become a significant concern because of the increasing infection rate and the catastrophic conse- quences of infection [15e17]. The treatment for bone cementerelated infection is however formidable, and the current resort of using antibiotics has created more hassles such as drug-resistance problems. Therefore, antiinfective bone cement without using antibiotics is highly desirable for orthopaedic surgery. In this regard, the osseointegrative, angiogenic and anti- infective properties, as well as low heat release from polymerization, is desirable for bone cement, and relevant modifications of PMMA along this line become mainstream research directions in this area. Here, a strategy of designing surface-degradable bone cements (SdBCs) is re- ported, and the biodegradable Mg was selected as the degrading component of SdBC, which reveals translational potential to meet the needs of osseointegration, angio- genesis, and anti-infection at the same time.

Bioactivity and biological properties of metallic Mg have recently been uncovered, and Mg alloys are designed as biodegradable materials primarily for orthopaedic applications [18e21]. This is largely due to elemental Mg being essential for bone development and metabolism and angiogenesis, which has also been reported in metallic Mg and its alloys [22e26]. Degradation of Mg and its alloys has also been reported to result in antibacterial effect due to the release of hydroxyl radicals and $Mg^{2þ}$ ions [27e29]. In addition, Mg and its alloy have tunable degradation rates *in vivo* [20,26]. Recent clinical studies have revealed the great translational po- tential of Mg alloys [30,31]. Thus, the present proof-of- concept study uses the aforementioned unique properties of Mg particles to modify clinically used PMMA bone cement, aiming at maintaining the feasibility of PMMA for MIOSs but simultaneously enhancing the bone/implant integration, angiogenesis and anti-infection performances

II. MATERIALS AND METHODS

Preparation of SdBC

PMMA bone cement and the commercially pure Mg particles (TangShan WeiHao Magnesium Powder Co., Ltd., Tangshan, China) with diam- eter of 100e150 mm were adopted for the preparation of SdBCs. In detail, 0.1, 0.2, 0.4 or 0.8 g of Mg particles were Mixed.

mixed with 2.6 g PMMA powder. Then, 1 mL of methyl- methacrylate (MMA) monomer was added in the mixed powder to form the SdBCs. The SdBCs were subsequently designated as 0.1-Mg, 0.2-Mg, 0.4-Mg and 0.8-Mg, the weight percentage of Mg particles being 2.7%, 5.3%, 10.2% and 18.4%, respectively. The PMMA was designated as 0-Mg for uniformity. Before the sample preparation, the Mg particles and OSTEOPAL V bone cement were kept at

T 23 1°C for 2 h. The distributions of C, O, Mg and Zr elements in the cements were characterized by scanning electron microscopy (SEM, JSM-7100F, JEOL Ltd., Japan) and energy-dispersive spectrometry .

In vitro degradation test

Cement cylinders with a diameter of 6 mm and height of 12 mm were immersed in Tris (tris(hydroxymethyl)amino- methane) buffer solution (pH Z 7.4) with the immersion ratio of 1.25 cm^2/mL at 37 °C for up to 60 days. The solution was replaced every 2 days. The weight change [(final weigh original weight)/original weigh00%] and pH of solution were monitored. The inner microstruc- ture and compressive properties of the bone cements before and after immersion were observed by SEM (Quanta 250, Thermo Fisher

— Scientific Inc., USA) and compressive

tests on a mechanical tester (HY10000; Shanghai HengYi Precision Instrument Co., Ltd., Shanghai, China) at 20 mm/ min, respectively. Before inner microstructure character- ization, the samples were successively polished up to 2000 grit finish and then cleaned. The surface morphology of SdBCs after immersion was also characterized by SEM. The hydrophilicity of the cement was evaluated using a water contact angle metre (DSA 25S; Zeiss, Germany).

Characterization of handling properties

The maximum temperature during polymerization, dough- ing time and setting time of the cement was tested in reference to ISO5833: 2002 standard. The doughing time was indicated by failure of the material to stick to the surface of a surgically gloved probing finger. For maximum- temperature measurements, the cement pastes were mixed and cast in a cylindrical mold. The change in tem- perature during the setting reaction was measured under ambient conditions at 23 °C. The setting time was calcu-

lated according to the following formula: Setting time Z (T_{amb} þ T_{max})/2, where T_{amb} is the ambient temperature and T_{max} is the maximum temperature.

Injectability was defined as the weight percentage of cement capable of getting injected out of the syringe at the doughing time with a constant loading at 50 N. For direct comparison, the injectability of SdBC was normalized by PMMA.

Cytocompatibility test

MC3T3-E1 osteoblasts from the Type Culture Collection of Chinese Academy of Sciences (TCC, CAS, Shanghai, China) were selected for the cytocompatibility tests. a-Minimum essential medium (HyClone Laboratories Inc., USA) with 10 vol % foetal bovine serum (HyClone) and 1 vol % penicillinestreptomycin solution were used as the cell culture medium. All the cells were cultured in a humidified atmosphere of 5% CO_2 at 37 $^{\circ}$C.

Cytocompatibility tests on material extracts The samples (with same dimensions) were immersed in 75% ethanol for 30 min for sterilization and then rinsed by phosphate buffer saline (PBS) 3 times to remove the ethanol. After that, the samples were immersed in the cell

culture media at an extraction ratio of 1.25 cm^2/mL at 37 $^{\circ}$C for 1 day. The supernatant was withdrawn and filtrated through 0.22-mm membrane filter (Millex-GP; Milli-pore) for cell tests. The cell culture media incubating at 37 $^{\circ}$C for 1 day was set as the control group.
Cells were cultured in material extracts at seeding density of 5000 cells/cm^2 for 1 and 3 days. Then, the cells were stained with LIVE/DEAD assay staining solution (Invitrogen™, Thermo Fisher Scientific Inc., USA) according to the manufacturer's instructions and then observed under a fluorescent microscope (EVOS, Thermo Fisher Scientific Inc., USA).
For cell counting kit-8 (CCK-8) assay, cells were cultured in 96-well plates in the presence of extracts for 1 and 3 days at a seeding density of 5000 cells/well. After prescribed times, the well was rinsed by 200 mL of PBS 2 times after removing the cell culture medium. Ten microlitres of CCK-8 (Dojindo Molecular Technologies, Inc) mixed in 100 mL of PBS was then added to each well and incubated at 37 $^{\circ}$C for 2 h. Then, the solution was transferred out to a new 96-well plate for optical density (O.D.) measurements on
a microplate reader (Power Wave X, BioTek Instruments, Inc., USA) at 450 nm. Cell viability Z $O.D._{Extract}/O.\ D._{Media}$ 100%.
The pH value and $Mg^{2þ}$ concentration of extracts before ✖
and after 1 and 3 days of cell culture were measured using a pH metre and atomic absorption spectrometer (AA800, Perkin Elmer), respectively.

Cell adhesion test
Before experiments, the samples (with same dimensions) were polished, cleaned and sterilized as described in sec- tion Cytocompatibility tests on material extracts. Then, the osteoblasts were cultured on these samples for 1 and 3 days at a seeding density of 5000 cells/cm^2. After that, the samples were gently rinsed with PBS and then fixed with 2.5% glutaraldehyde for 4 h. Then, the samples were dehydrated with a series of ethanol solutions and finally dried using the critical point drying equipment (CPD300; Leica Instrument Co., Ltd., Germany) for SEM observation. The pH values of cell culture media after direct-contact cell culture for 1 and 3 days were measured.

in the presence of various extracts at a seeding density of 5000 cells/cm^2. The extracts were prepared using the DMEM-based cell culture media as described in section Cytocompatibility tests on material extracts. After 18 h, the tube formation was observed with an inverted phase contrast microscope (Axiocam 503; Carl Zeiss Co., Ltd., Germany). The images were analyzed using ImageJ (Na- tional Institutes of Health, USA) with the Angiogenesis Analyzer plugin to quantify the number of nodes, tubes and total length of network, per square millimetre.

Bacteria adhesion test
Staphylococcus aureus (*S. aureus* ATCC 25923) and *Escher- ichia coli* (*E. coli* ATCC 25922) were adopted in the test. The bacterial cells were propagated on an agar plate for 18e24 h at 37 $^{\circ}$C to create colony-forming units (CFUs). One CFU from the plate was inoculated in Luria broth (LB) media to prepare bacterial suspensions, which were cultured in a shaking incubator at 190 rpm and 37 $^{\circ}$C for 16e18 h, and then diluted with LB media for O.D. measurement at a wavelength of 670 nm to identify bacteria density in reference to the standard curve. Finally, the bacterial suspension was diluted with LB media to be 2.38 10^6 CFU/
mL.
Samples (with same dimensions) were sterilized as de- scried in section Cytocompatibility tests on material extracts. Then, 1 mL of diluted bacterial suspension was added to the samples in the 24-well plate and incubated at 37 $^{\circ}$C and 5% CO_2. After 24 h, the samples ✖ were fixed and dehydrated as described in section Cell adhesion test for SEM characterization. Four parallel samples were observed for each kind of bacteria.

In vivo study

The animal test plan and institutional ethical use protocols were approved by the ethics committee of the institutes the authors of the study are affiliated to. Six male SpragueeDawley rats (weight, 400 20 g) were used. All surgeries were performed under standard anaesthesia and disinfection procedures. Transcortical holes with a diam- T
eter of 2 mm were drilled at the position of all femoral diaphysis under irrigation with saline after skin incision (1e2 cm long). 0-Mg and 0.2-Mg sample cylinders with a diameter of 1.9 mm and height of 8 mm were inserted into the holes of left and right femur, respectively. Finally, the incision was closed and animals were housed individually with normal access to food and water.

The rats were sacrificed at 2 months, and the retrieved tissue samples with implants were scanned using a microecomputed tomography (CT) scanner (Skyscan 1176; Bruker microCT) at an isometric resolution of 17 mm. The results were analyzed using the built-in analysis software. Owing to the similar contrast between bone and implant, the new bone formation was evaluated qualitatively through morphological analysis on three-dimensional (3D) reconstruction images.

Immediately after micro-CT analysis, half of specimens in each group were fixed in 4% paraformaldehyde for 2 days and then dehydrated and embedded in epoxy resin for SEM observation. The other half specimens were mounted on a test fixture for the push-out test at a displacement rate of 0.5 mm/min at a moist condition. The femur specimens after the push-out test were fixed in 4% paraformaldehyde for 2 days and then decalcified in ethylenediaminetetraacetic acid solution for histological analysis. Tissue sections (6-mm thick) were stained, respectively, by haematoxylineeosin (H&E) and Masson trichrome staining method for transmitted light microscopy (AxioCam HRc; Zeiss) observation.

Statistical analysis

These measurements were run in at least three duplicates, and results were reported as the mean standard devia- tion calculated from repeated measurements. Statistical analysis of the cell proliferaTion results and endothelial tube formation results was conducted by one-way analysis of variance. All the pair-wise comparisons were performed by the *post hoc* test of Turkey. The two-tailed two-sample *t* test was used for the statistical analysis of push-out test results. When a p value was less than 0.05, significant dif- ferences were determined.

III. RESULTS

Surface degradation behaviour of SdBCs

Addition of Mg particles did not affect the monomer poly- merization of acrylic cement. After the cement was completely set, Mg particles appeared to evenly distribute in the PMMA matrix according to the SEM (Fig. 1A) and element distribution observation (Fig.S1), leading to ho- mogeneous mechanical, degradation and biological prop- erties of SdBCs. After immersion for 60 d, the interior of the SdBCs kept intact (Fig. 1A) because of no contacting with fluids, indicating that the Mg particles embedded inside the PMMA matrix would be a permanent second phase of the composite cement as expected, which is beneficial for preserving mechanical strength and tissue compatibility of the cement in the long-term implantation. In contrast, a great number of voids and pores were formed on the sur- face (Fig. 1B), of which the number increased with the in- crease of Mg content, confirming the surface-degradable property of the SdBCs. More importantly, the uniform dis- tribution of Mg particles caused even surface degradation, indicating that the void size and density on the bone cement surface could be precisely controlled.

The surface degradation behaviour of SdBC was quanti- tatively confirmed by the weight loss of the samples (Fig. 1C). The percentage of weight loss was 0.3%, 2.3%, 2.6% and 5.7% for 0.1-Mg, 0.2-Mg, 0.4-Mg and 0.8-Mg, respectively, and all are much lower than the original weight percentage of Mg in each SdBC, indicating that only the Mg particles on the cement surface degraded. In addi- tion, degradation of SdBCs slowed down gradually, probably because of the gradual loss of Mg on the cement surface and the protection formed by its degradation products [32,33]. The surface degradation behaviour of SdBCs also affected the chemical microenvironment adjacent to the cement. As a result of Mg degradation, the alkalinity was significantly altered as elevated pH values was observed in

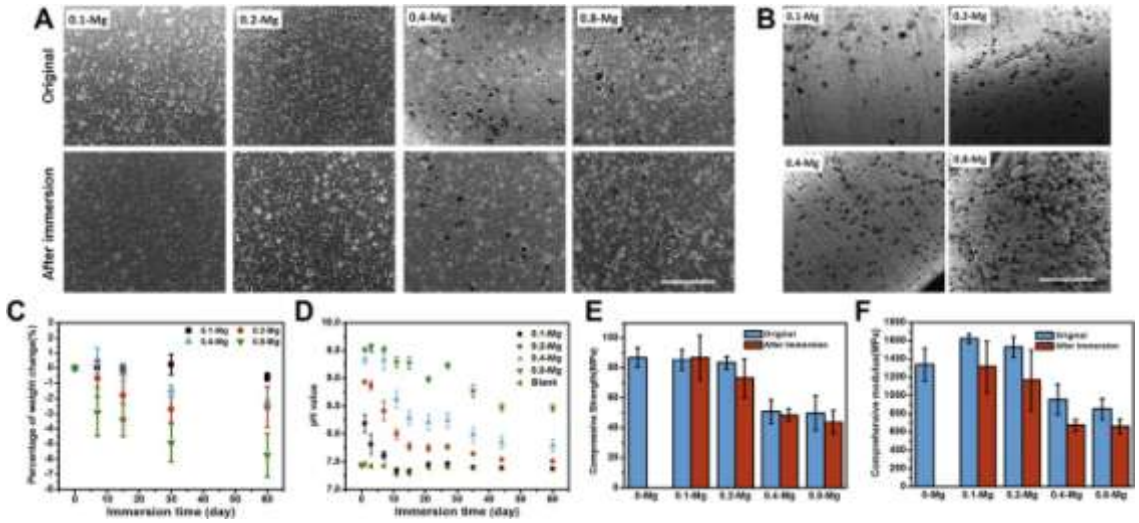

Figure 1 Surface degradation behavior of SdBCs. (A) SEM images of SdBCs before and after immersion in Tris solution for 60 d. The small white dots in the images are zirconium particles in the OSTEOPAL V bone cement as X-ray opaque agents. Scale bar, 1 mm. (B) Surface morphologies of SdBCs after immersion. Scale bar, 1 mm. (C) Percentage of weight change of SdBCs and (D) pH values of the immersion solution during immersion test. (E) Compressive strength and (F) compressive modulus of PMMA bone cement and SdBCs before and after immersion.

PMMA Z poly(methylmethacrylate); SdBCs Z surface-degradable bone cements; SEM Z scanning electron microscopy.

the immersion fluid with SdBCs and correlated to the Mg content released (Fig. 1D).

Surface degradation of SdBCs however did not cause dramatic decrease in the compressive strength of cements (Fig. 1E). The decrease in the compressive strengths of SdBCs with the increasing initial content of Mg was probably due to the increased void density and the weakened Mg particle/PMMA interface strength [34]. The conservation of compressive strength during degradation is very important for load-bearing applications in orthopaedics and is a main advantage of the surface-degradable implant compared with the completely degradable cements such as calcium sulfates.

The greater compressive moduli of 0.1-Mg and 0.2-Mg compared to those of PMMA bone cement (Fig. 1F) should be attributed to the much higher modulus (w45 GPa) of metallic Mg than that of PMMA, agreeing with previous studies [35,36], while the lower compressive moduli of 0.4- Mg and 0.8-Mg compared to those of PMMA is probably due to the high density of voids in these SdBCs. The surface degradation of SdBCs decreased their compressive moduli and not compressive strength (Fig. 1F), which is beneficial for alleviating stress-shielding effect [37] or the secondary vertebra fracture when used for PKP [38].

Handling properties and hydrophilicity of SdBCs

The handling properties of the bone cement are crucial for minimally invasive surgical operation and the efficacy of PKP or percutaneous vertebroplasty (PVP). The doughing time and setting time of SdBCs were both lower than those of PMMA. When increasing the content of Mg, the doughing times of SdBCs decreased while the setting time first

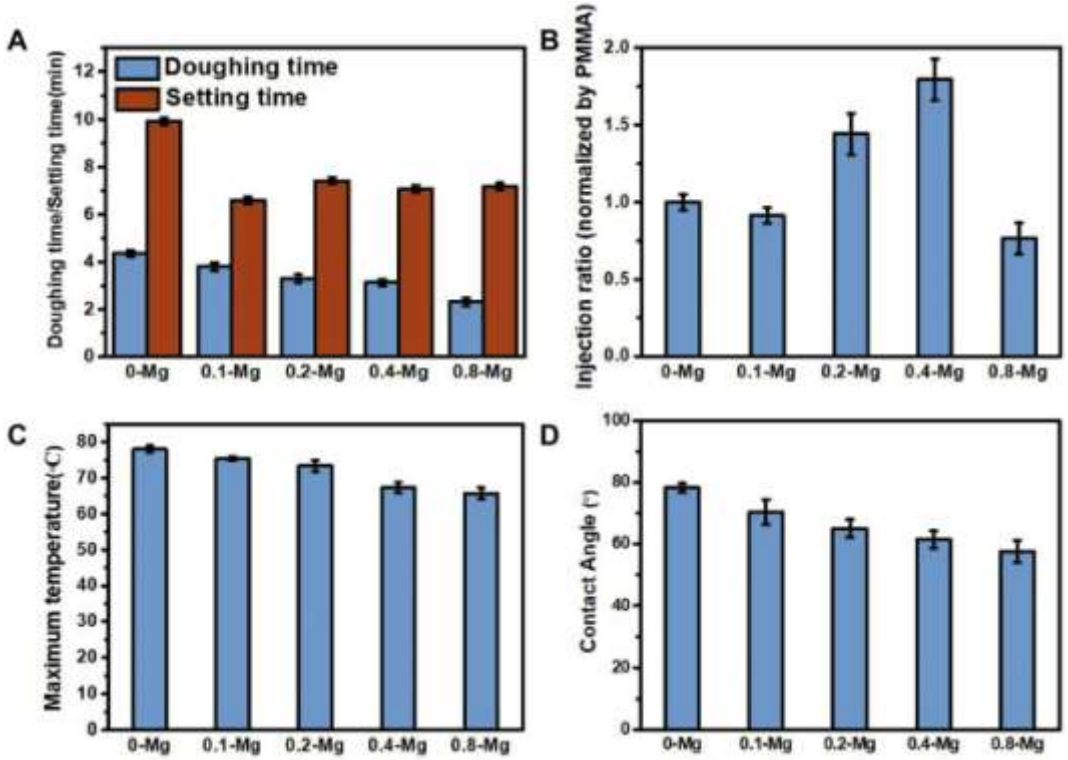

Figure 2 Handling properties and surface wettability of SdBCs. (A) Initial and final setting time and (B) injection ratio of PMMA and SdBCs. (C) Maximum temperature during polymerization of PMMA and SdBCs. (D) Water contact angle on PMMA and SdBCs. PMMA Z poly(methylmethacrylate); SdBCs Z surface-degradable bone cements.

Owing to surface degradation, the pH value and $Mg^{2þ}$ concentration of SdBC extracts significantly increased with the increase in Mg content of SdBCs (Fig. 3C and D). When used for cell culture, the pH values of all extracts decreased and the difference among the groups narrowed after 1 or 3 d. However, the $Mg^{2þ}$ concentration of each extract remained almost unchanged after cell culture. These results indicate that the decrease of cell viability from 0.1-Mg to 0.8-Mg at 1 d should be due to the acute toxic effects of high pH value rather than the high $Mg^{2þ}$ concentration of the extracts. In addition, the good cell viability of 0.4-Mg and 0.8-Mg groups at 3 d should be attributed to both the properly high $Mg^{2þ}$ concentration [42,43] and the decrease of pH (to a proper value that supports osteoblast proliferation [44]) of extracts in these groups.

The decreased cell viability with increasing Mg content at 1 d is probably due to the acute toxic effects of high pH values of the extracts, while the later increased cell pro- liferation at 3 d could be attributed to the gradually increased $Mg^{2þ}$ concentration and reduced pH value of the extracts.

SEM observation clearly showed that all osteoblasts on SdBCs exhibited better adhesion and spreading than the cells on PMMA at 1 d (Fig. 4A), which is consistent with the results reported in the previous work of poly(lactic-co-gly- colic)/Mg alloy composite [45].

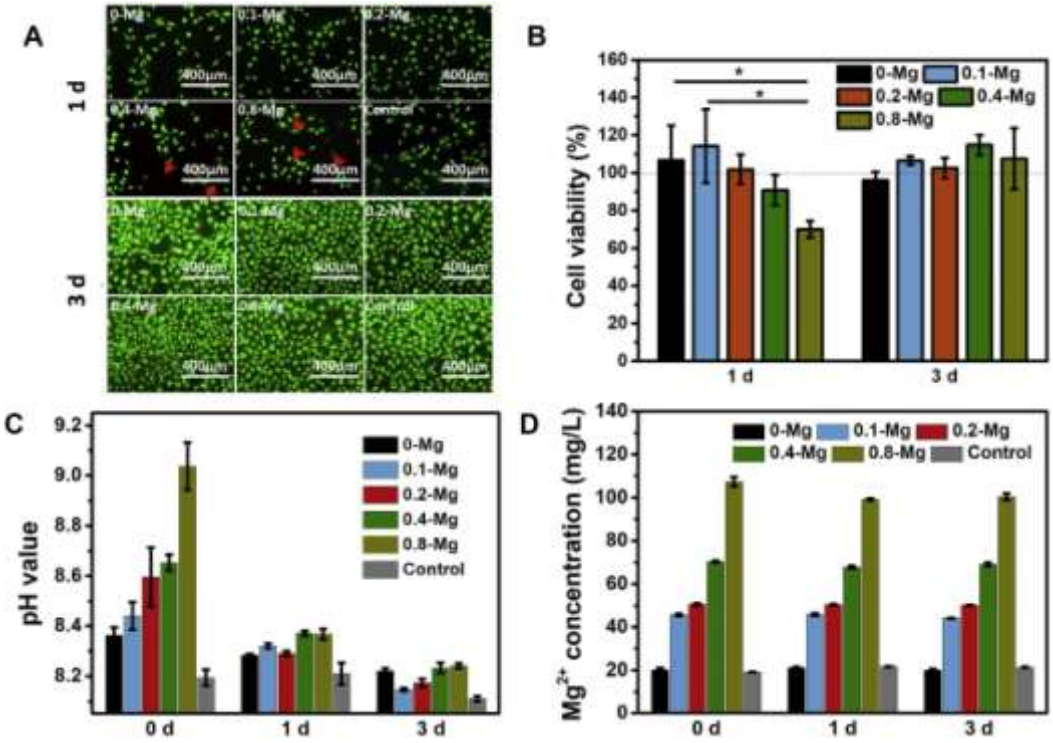

Figure 3 Cell viability in various material extracts. (A) Fluorescence micrographs of LIVE/DEADestained osteoblasts after cultured in different extracts for 1 and 3 d. The red arrows indicate dead cells. (B) Cell viabilities of different groups at 1 and 3 d.
(C) pH value and (D) Mg^{2p} concentration of extracts before and after cell culture for 1 and 3 d.

significantly lowered than that on PMMA, and in fact, there were almost no bacterial aggregates on the SdBCs. The bacterial inhibitory effect of SdBCs against *S. aureus* was enhanced with the increasing Mg content in the cement, while interestingly, the inhibitory effect against *E. coli* was not significant and only 0.8-Mg showed obviously higher bacterial reduction than PMMA.

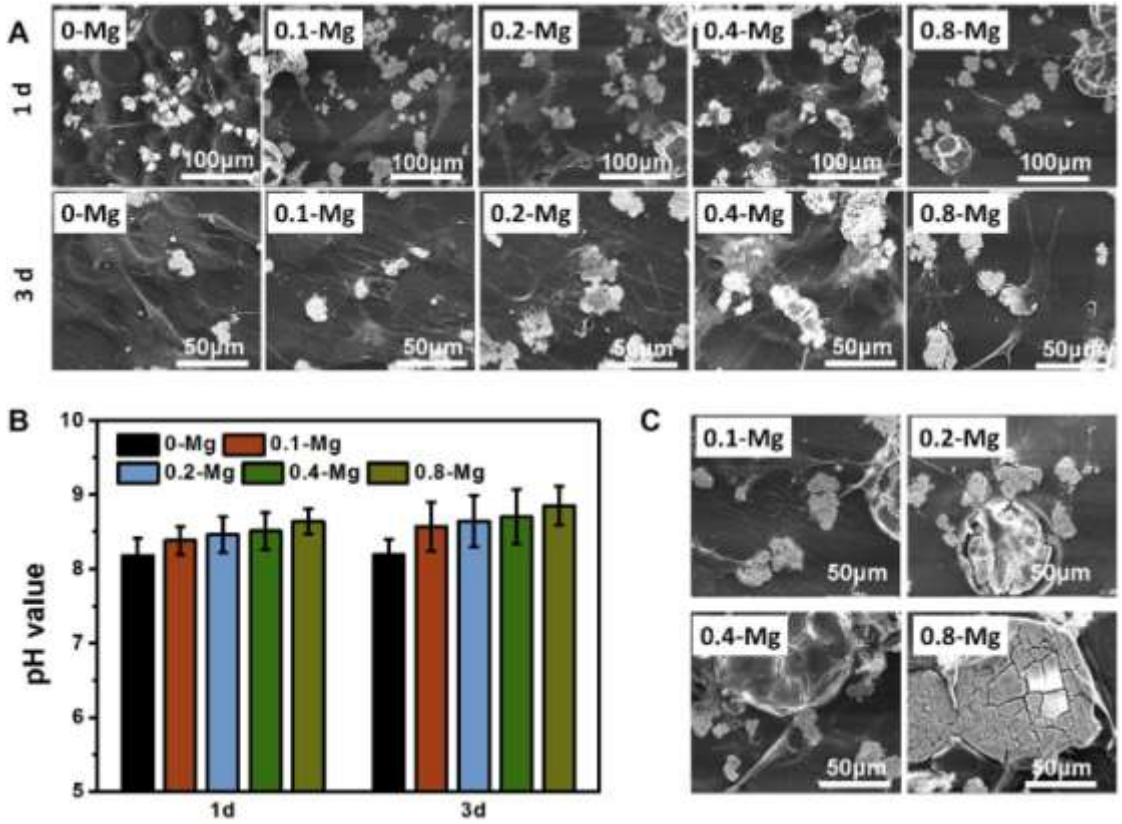

Figure 4 Cell spreading and viability on various samples. (A) Morphology of osteoblasts on the pristine PMMA bone cement and different SdBCs at 1 and 3 d. (B) pH of cell culture media after culturing for 1 and 3 d. (C) Morphology of osteoblasts on and around Mg particles in SdBCs at 1 d.
PMMA Z poly(methylmethacrylate); SdBCs Z surface-degradable bone cements.

nondegradable and injectable acrylic bone cement. SdBC owns several advantages compared with the totally degradable or noninjectable bone cements and is suitable for various orthopaedic surgeries, especially minimally invasive ones.

Unlike the totally degradable cements, surface- degradable characteristic of SdBCs benefits the mainte- nance of excellent mechanical strength (Fig. 2D) *in vivo*, which is critical for load-bearing applications. The compressive modulus of SdBCs could decrease by about 20% after degradation (Fig. 1F), which could alleviate stress-shielding effects [37] of stiff PMMA or the secondary vertebra fracture usually caused by acrylic cements in PKP [38].

Degradation of Mg particles at the surface of SdBCs releases hydroxyl, $Mg^{2þ}$ and H_2 gas and alters the surface morphology and chemical composition of SdBCs. These factors will synergistically affect the biological response to the cement, and this mechanism is lacking in the nondegradable cements. First, osteoblasts adhered and spread better on the 0.1-Mg and 0.2-Mg samples than on the PMMA (Fig. 3A), which should be attributed to the proper $Mg^{2þ}$ concentration around these SdBCs and the CaP and MgP deposition on the SdBC surface, both facili- tating osteoblast growth [48].

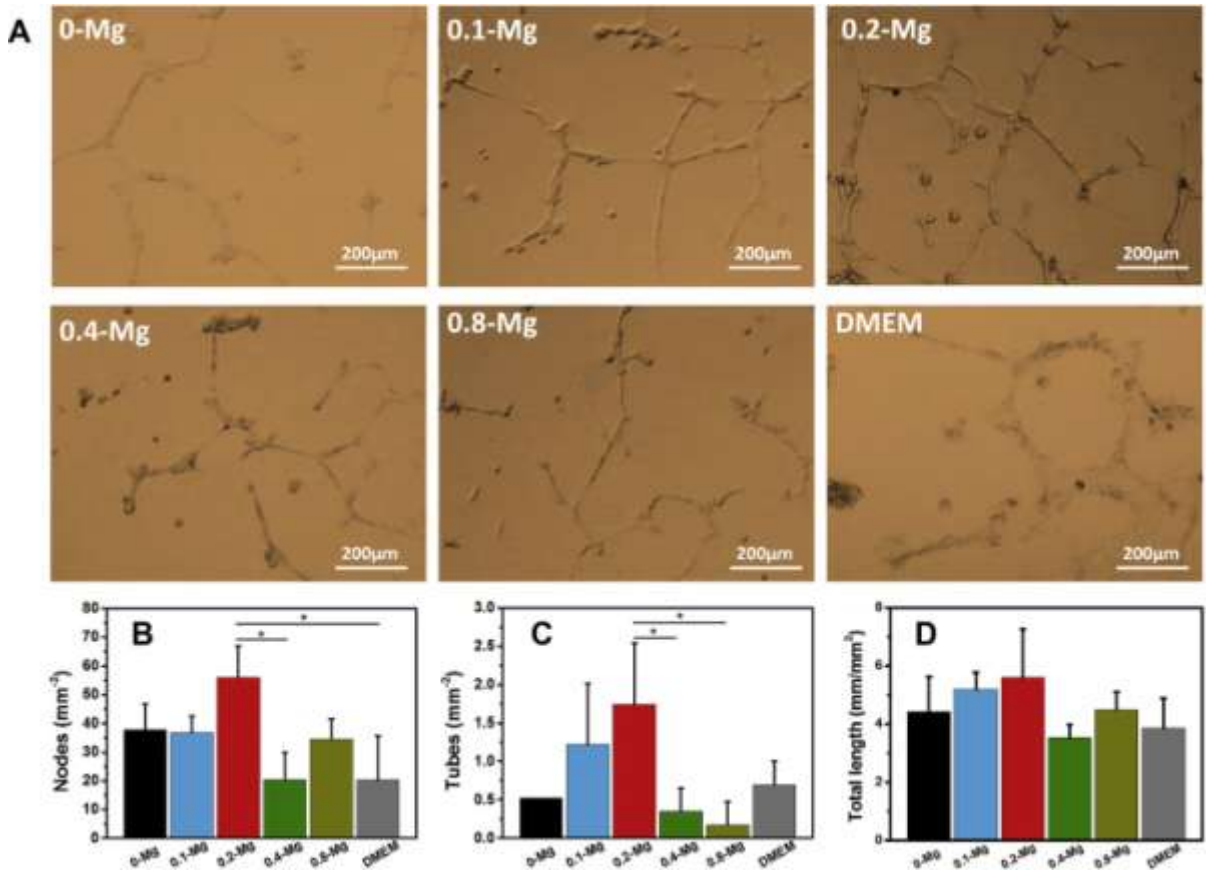

Figure 5 *In vitro* angiogenesis of HUVECs cultured on the Matrigel basement membrane matrix in the presence of different extracts at 18 h. (A) Typical images in different groups. (B) The number of tubes, (C) number of nodes and (D) total length of network, per square millimetre.
HUVECs Z human umbilical vein endothelial cells.

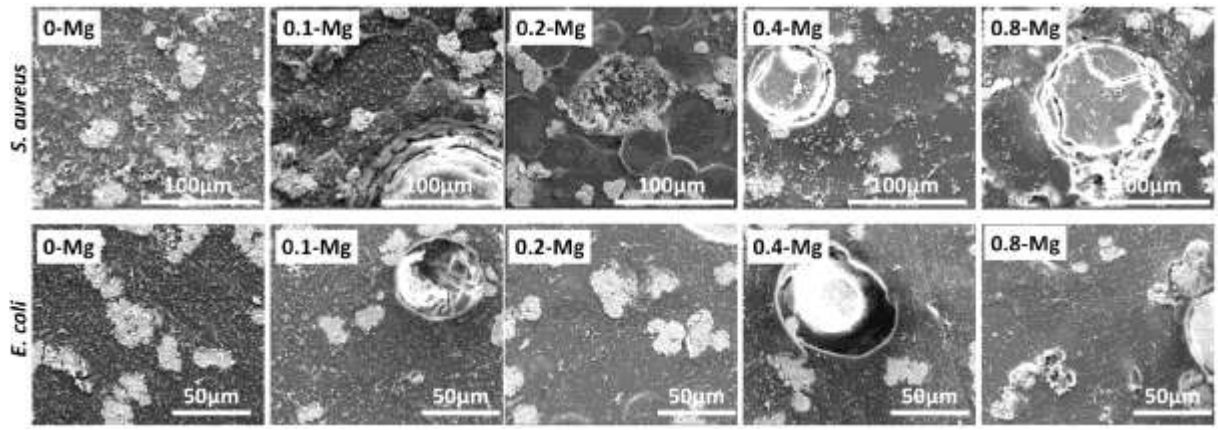

Figure 6 *S. aureus* and *E. coli* adhesion on various samples at 24 h observed by SEM. SEM Z scanning electron microscopy.

physical interlocking eventually. The high interface strength is important for long-term stability of the bone/ implant interface. The bone/cement interface strength of 0.2-Mg SdBC measured by push-out force was significantly higher than that of PMMA, suggesting a strong physical interlocking mechanism between bone and SdBC, as well as enhanced bone formation and osseointegration. The

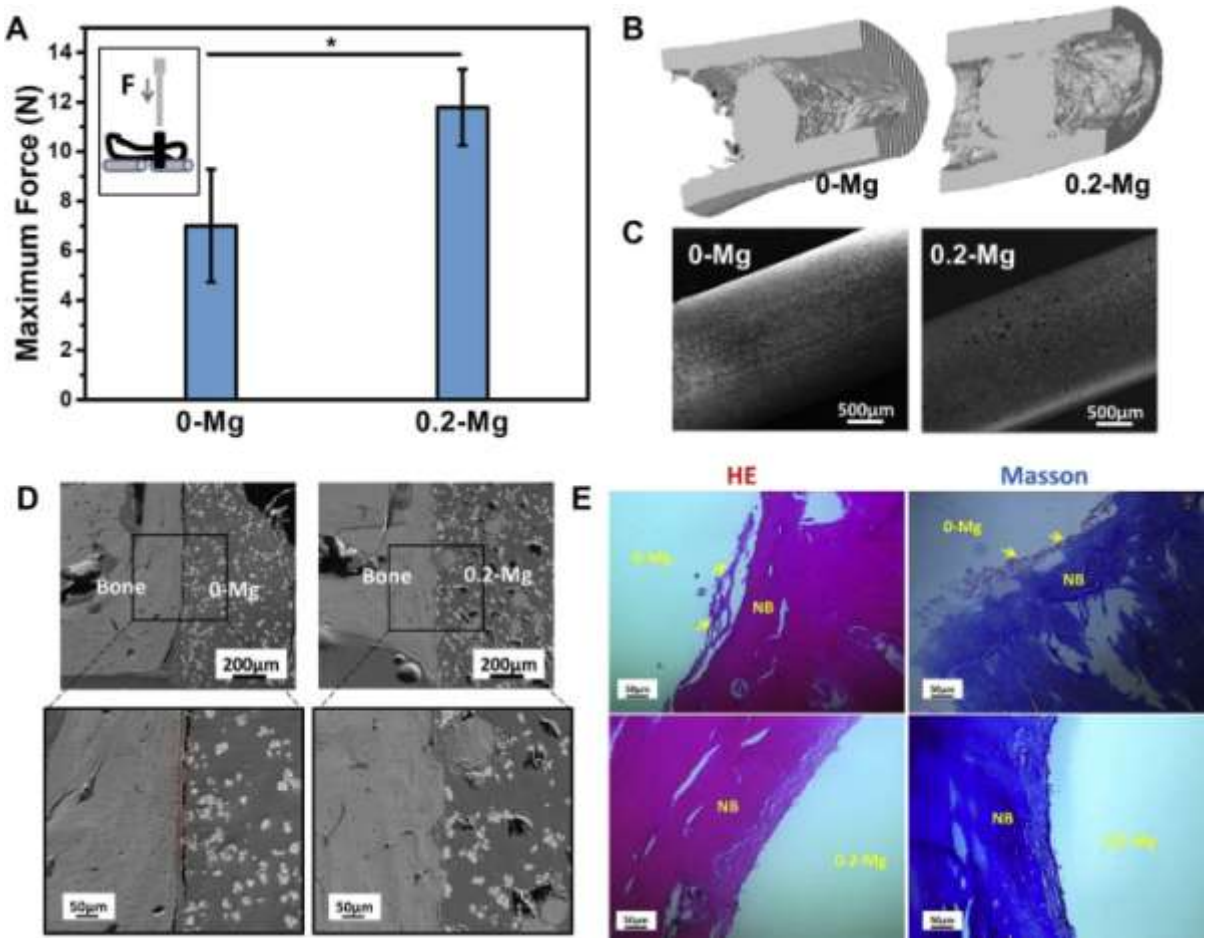

Figure 7 *In vivo* bone response evaluations. (A)Maximum force obtained from biomechanical push-out test. The inset shows setup for push-out test. *, $p < 0.05$. (B) 3D micro-CT images of the femur around implant obtained from the longitudinal viewpoint at 2 m of implantation. (C) Surface morphology of samples and (D) bone/implant interface morphology at 2 m of implantation, observed by SEM. (E) H&E-stained and Masson trichromeestained slices of periimplant bone tissue at 2 m. NB Z new bone. "0-Mg" and "0.2-Mg" indicate the initial implant site. Arrows point the fibrous capsule.
CT Z computed tomography; H&E Z haematoxylineeosin; SEM Z scanning electron microscopy.

setting time) is essential for appropriate handling and deployment of cements, and typically, the surgeon needs 6e8 min to mix and inject the cement in PVP [57]. SdBCs had acceptable setting times for minimally invasive sur- gery, and typical setting time was between 6.6 and 7.4 min.

In addition, the injectability of 0.1-Mg, 0.2-Mg and 0.4-Mg would meet the requirement for clinical use and the improvement of injectability by adding 5.4 wt% to 10.3 wt% of Mg particles, agreeing with previous studies [12,58]. The reduction of potentially harmful high temperature during PMMA polymerization by adding Mg particles is another important advantage of SdBCs [3].

Although the present study exhibits many advantages of SdBC, it should be optimized to meet the clinical re- quirements of MIOS, including the handling, materials and biological properties, especially the angiogenic and anti- bacterial capabilities. The Mg particle concentration greatly influences the handling and material properties of SdBC, and another factor could be the size of Mg particles.

osteogenic, angiogenic and antibacterial properties [41,52e54] should be adopted. Degradation rate [20] and size of Mg particles should be optimized to promote bone ingrowth on SdBCs [59]. Future directions should be focused on the optimization of the composite bone cements by adjusting the content, size and composition of Mg particles. Long-term *in vivo* study was also necessary to evaluate the long-term bone/implant interface, local bone response and systematic biosafety.

IV. CONCLUSIONS

The present study demonstrated a novel and effective strategy of developing surface-degradable PMMA/Mg bone cements that possess environmentally responsive surface, leading to a porous surface for bone ingrowth while pre- serving the high compressive strength of acrylic cement. The surface-degradation induced by Mg particles creates a proper ionic vicinity around the bone cement, which pro- motes osteoblasts activity and tube formation of HUVECs and inhibits bacterial adhesion on the cement surface.

REFERENCES

[1]. Ali U, Karim KJ, Buang NA. A review of the properties and applications of poly (methyl methacrylate) (PMMA). Polym Rev2015;55(4):1e28.
[2]. He Z, Zhai Q, Hu M, Cao C, Wang J, Yang H, et al. Bone cements for percutaneous vertebroplasty and balloon kyphoplasty: current status and future developments. J Orthop Translat 2015;3(1):1e11.
[3]. Castaldini A, Cavallini A. Setting properties of bone cement with added synthetic hydroxyapatite. Biomaterials 1985;6(1): 55e60.
[4]. Sundfeldt M, Carlsson LV, Johansson CB, Thomsen P,Gretzer C. Aseptic loosening, not only a question of wear: areview of different theories. Acta Orthop 2006;77(2):177e97.
[5]. Lewis G. Properties of acrylic bone cement: State of the artreview. J Biomed Mater Res B 1997;38(2):155e82.
[6]. Ries MD, Young E, Al-Marashi L, Goldstein P, Hetherington A,Petrie T, et al. In vivo behavior of acrylic bone cement in totalhip arthroplasty. Biomaterials 2006;27(2):256e61.
[7]. Goodheart JR, Miller MA, Mann KA. In vivo loss of cement-bone interlock reduces fixation strength in total knee arthroplasties.J Orthop Res 2014;32(8):1052e60.
[8]. Heo SJ, Park SA, Shin HJ, Lee YJ, Yoon TR, Seo HY, et al.Evaluation of bonding stress for the newly suggested bone cement: comparison with currently used PMMA through animal studies. Key Eng Mater 2007;342-343:373e6.
[9]. Wolf-Brandstetter C, Roessler S, Storch S, Hempel U,Gbureck U, Nies B, et al. Physicochemical and cell biologicalcharacterization of PMMA bone cements modified with additives to increase bioactivity. J Biomed Mater Res B 2013;101B(4):599e609.
[10]. Khandaker M, Li Y, Morris T. Micro and nano MgO particles for the improvement of fracture toughness of bone-cement interfaces. J Biomech 2013;46(5):1035e9.
[11]. Tan H, Guo S, Yang S, Xu X, Tang T. Physical characterization and osteogenic activity of the quaternized chitosan-loaded PMMA bone cement. Acta Biomater 2012;8(6):2166e74.
[12]. Kim SB, Kim TJ, Yoon TL, Su AP, Cho IH, Kim EJ, et al. The characteristics of a hydroxyapatiteechitosanePMMA bone cement. Biomaterials 2004;25(26):5715e23.
[13]. Cimatti B, Santos MA, Brassesco MS, Okano LT, Barboza WM,Nogueirabarbosa MH, et al. Safety,osseointegration, and bone ingrowth analysis of PMMA-based porous cement on animal metaphyseal bone defect model. J Biomed Mater Res B 2017; 106(10):649e58.
[14]. Brey EM, King TW, Johnston C, Mcintire LV, Reece GP, Patrick Jr CW. A technique for quantitative three-dimensional analysis of microvascular structure. Microvasc Res 2002;63(3): 279e94.
[15]. Hendriks JG, van Horn JR, van der Mei HC, Busscher HJ. Backgrounds of antibiotic-loaded bone cement and prosthesisrelated infection. Biomaterials 2004;25(3):545e56.
[16]. Ridgeway S, Wilson J, Charlet A, Kafatos G, Pearson A, Coello R. Infection of the surgical site after arthroplasty of the hip. J Bone Joint Surg Br 2005;87(6):844e50.
[17]. Ying Y, Ao H, Wang Y, Lin W, Yang S, Zhang S, et al. Cytocompatibility with osteogenic cells and enhanced in vivo antiinfection potential of quaternized chitosan-loaded titania nanotubes. Bone Res 2016;4(3):140e53.
[18]. Staiger MP, Pietak AM, Huadmai J, Dias G. Magnesium and its alloys as orthopedic biomaterials: a review. Biomaterials2006;27(9):1728e34.
[19]. Witte F. The history of biodegradable magnesium implants: areview. Acta Biomater 2010;6(5):1680e92.
[20]. Zheng Y, Gu X, Witte F. Biodegradable metals. Mater Sci Eng R2014;77(2):1e34.
[21]. Lin X, Tan L, Wang Q, Zhang G, Zhang B, Yang L. In vivodegradation and tissue compatibility of ZK60 magnesium alloy with micro-arc oxidation coating in a transcortical model. Mater Sci Eng C-Mater 2013;33(7):3881e8.

[22]. Witte F, Kaese V, Haferkamp H, Switzer E, Meyer-Lindenberg A, Wirth CJ, et al. In vivo corrosion of four magnesium alloys and the associated bone response. Biomaterials 2005;26(17):3557e63.
[23]. Castellani C, Lindtner RA, Hausbrandt P, Tschegg E, Stanzl- Tschegg SE, Zanoni G, et al. Bone-implant interface strength and osseointegration: biodegradable magnesium alloy versus standard titanium control. Acta Biomater 2005;7(1):432e40.